Structural Engineering and Mechanics, Vol. 4, No. 1 (1996) 37-47
DOI: http://dx.doi.org/10.12989/sem.1996.4.1.037

Elastic distortional buckling of overhanging beams

M.A. Bradford †

Department of Structural Engineering, School of Civil Engineering
The University of New South Wales, Sydney, NSW 2052, Australia

Abstract. The paper considers the elastic distortional buckling of overhanging beams, which consist of an internal segment with a cantilevered segment continuous over an internal support. The beams were considered loaded by a concentrated load at the cantilever tip, and the beams were either partially restrained or laterally restrained over the internal support. An efficient line-type finite element developed previously by the author was modified to incorporate loading remote from the shear centre, as well as to allow for lateral buckling without distortion. Buckling loads were obtained for a range of geometry when the load was placed on the top flange, at the shear centre or on the bottom flange. Buckling mode shapes were also obtained, and conclusions drawn regarding the influence of distortion on the overall buckling load.

Key words: buckling; distortion; elasticity; modes; overhanging beams;

1. Introduction

The overall buckling mode in I-section beams is generally assumed to be lateral-torsional (Trahair and Bradford 1991), based on the usual Vlasov assumption that the beam's cross-section remains rigid during buckling. However, when the assumption of a rigid cross-section is relaxed, the buckling mode is known as lateral-distortional (Hancock *et al.* 1980). Lateral-distortional buckling modes may be thought of as being a coupling between local and lateral buckling, where the buckling half-wavelength is much greater than the order of the cross-section dimensions.

Research work on lateral-torsional buckling has been very extensive, as indicated by a recent monograph on the phenomenon by Trahair (1993). A state of the art publication by the author (Bradford 1992a) showed that far less attention had been devoted to the study of lateral-distortional buckling, although computer-oriented approaches have made analyses of lateral-distortional buckling far more tractable. Generally, distortion of simply supported members occurs during the buckling of beams with slender webs and narrow stocky flanges, or when a beam is partially restrained, as occurs with the seat support shown in Fig. 1 (Bradford 1989).

The degree by which the lateral-distortional buckling load of a simply supported beam falls below its lateral-torsional buckling load is not large for practical beam dimensions, while a recent study (Bradford 1992b) has shown that the reduction in buckling load due to distortion may be significant for cantilevers, particularly if loaded above the shear centre. A transition between a simply supported beam and a cantilever is an overhanging beam, as shown in Fig. 2. The lateral buckling of such beams has been considered by Trahair (1983), but the treatment of lateral-distortional buckling of overhanging beams appears to have been considered nowhere

† Associate Professor

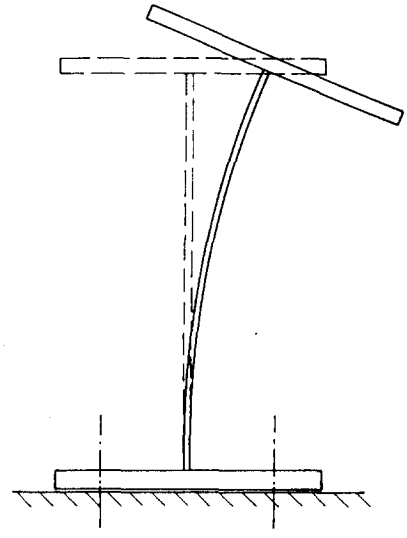

Fig. 1 Partial restraint at a seat support

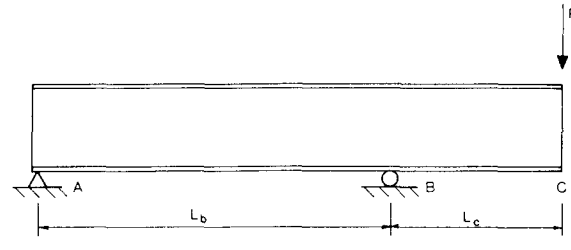

(a) Beam

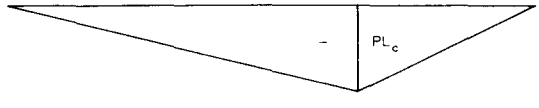

(b) Bending moment diagram

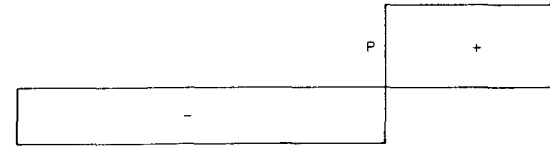

(c) Shear force diagram

Fig. 2. Overhanging beam

in the open literature.

This paper therefore studies the elastic lateral-distortional buckling of overhanging beams, using the computationally efficient "Bradford-Trahair" line finite element developed by Bradford and Trahair (1981). This element, as described in the latter publication, is augmented here to allow for concentrated loads remote from the shear centre, and a modification of the elastic and geometric stiffness matrices is described which allows for the suppression of distortion so that lateral-torsional buckling loads may be predicted. Two different restraint conditions over the internal support (B in Fig. 2) are considered, and lateral-torsional and lateral-distortional buckling loads are calculated for a concentrated load at the free end of the cantilever segment. The buckling loads, as well as the mode shapes, are used to quantify the effects of distortion on overall buckling.

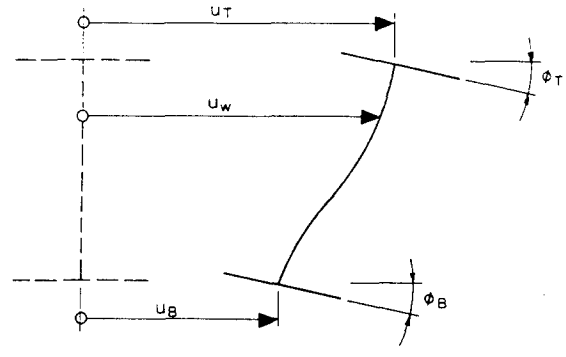

(a) Buckling deformations

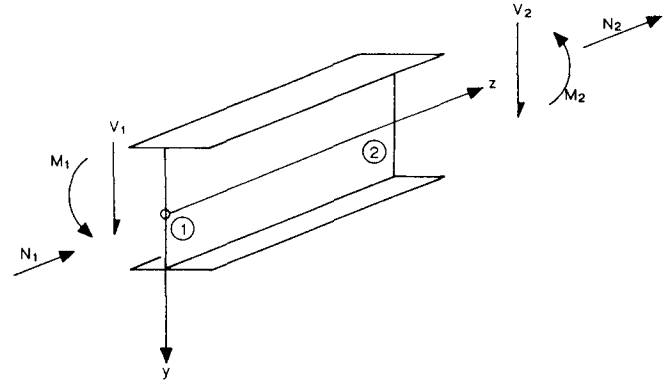

(b) Element and actions

Fig. 3. Bradford-Trahair element

2. Finite element analysis

2.1. General

The Bradford-Trahair element deployed for the distortional buckling study is shown in Fig. 3. It is a "beam" or "line" type element into which the member is discretised longitudinally. Details of the derivation of the elastic and geometric stiffness matrices are given by Bradford and Trahair (1981).

The main assumptions used in producing the line element are:

(1) the steel is linearly elastic;
(2) the effect of major axis deformations can be neglected in the buckling analysis;
(3) the two flanges are stocky enough to displace and twist as rigid bodies;
(4) the web is flexible, and distorts as a cubic curve in the plane of its cross-section during buckling; and
(5) the loading is initially in the plane of the web, and remains vertical during buckling (ie. conservative loads).

The buckling displacements u_T, u_B, ϕ_T and ϕ_B in Fig. 3 are assumed to be cubic functions

of the longitudinal coordinate z, and can be written in terms of the vector of element distortional buckling displacements

$$\{q_d\}=\langle u_{T1},\ u_{T2},\ u'_{T1},\ u'_{T2},\ u_{B1},\ u_{B2},\ u'_{T1},\ u'_{T2},\ \phi_{T1},\ \phi_{T2},\ \phi_{B1},\ \phi_{T2}\rangle^T \tag{1}$$

where primes denote differentiation with respect to z.

By using displacement and slope compatibility at the flange-web junctions, the web buckling displacements u_W may also be written as

$$u_W=\langle N_W\rangle\ \{q_d\} \tag{2}$$

where $\langle N_W\rangle$ is a cubic interpolation vector in y and z. The beam or line element thus has 12 degrees of freedom, six at each end.

Strain energy U^e is stored in the element during buckling, which may be written as

$$U^e=\frac{1}{2}\langle q_d\rangle\ [k]\ \{q_d\} \tag{3}$$

where $[k]$ is the 12×12 elastic stiffness matrix given by Bradford and Trahair (1981).

Similarly, the actions M, V and N acting on the element in Fig. 3 are increased monotonically by a load factor λ until buckling takes place. These actions do work V^e, which can be expressed as

$$V^e=\frac{1}{2}\lambda\langle q_d\rangle\ [g]\ \{q_d\} \tag{4}$$

where $[g]$ is the 12×12 geometric or stability matrix of the element given by Bradford and Trahair (1981).

By using a suitable assembly routine based on equilibrium and compatibility at the nodes, the total potential Π may be written as

$$\Pi=\frac{1}{2}\langle Q_d\rangle\ ([K]-\lambda[G])\ \{Q_d\} \tag{5}$$

where $[K]$ and $[G]$ are the member stiffness and stability matrices respectively, assembled from $[k]$ and $[g]$, while $\{Q_d\}$ is the vector of buckling degrees of freedom assembled from $\{q_d\}$ for each element. Minimising the total potential Π with respect to the distortional buckling displacements $\{Q_d\}$ produces

$$\frac{\partial\Pi}{\partial\{Q_d\}}=([K]-\lambda[G])\ \{Q_d\}=\{0\} \tag{6}$$

Since the buckling displacements $\{Q_d\}$ are nonzero, the solution to Eq. (6) is

$$|[K]-\lambda[G]|=0 \tag{7}$$

which represents a standard linear eigenproblem. Eq. (7) may be solved for the buckling load factor λ by invoking standard eigenvalue routines (Ronagh and Bradford 1996), while the corresponding value of $\{Q_d\}$ in Eq. (6) is the eigenvector or normalised buckled shape.

2.2. Modification for concentrated loads remote from the shear centre

It is well-known that when a concentrated load P acts at a height $\overline{a}$ aove the shear centre

of a beam, the lateral buckling resistance is lowered because of the additional disturbing torque $P\bar{a}\phi$ which increases the twisting of the beam (Trahair 1993). This effect can easily be allowed for by the augmenting the stability matrix for the element by including the term $1/2\,\lambda\ P\bar{a}\phi^2$ in the expression for the element work done V^e if the cross-section is not being distorted.

For the case of lateral-distortional buckling when the load λP_1 at element node 1 acts within the web at a height $\bar{a}_c$ above the shear centre, the load point is lowered due to deformation of the web at this node, $(u_w)_{z=0}$, by

$$\frac{1}{2}\int_0^{\bar{a}_c}\left(\frac{\partial u_w}{\partial y}\right)^2_{z=0} dy$$

so that the loss in potential V_c^e is given by

$$V_c^e=\frac{\lambda P_1}{2}\int_0^{\bar{a}_c}\left(\frac{\partial u_w}{\partial y}\right)^2_{z=0} dy \tag{8}$$

Substituting Eq. (2) into Eq. (8), the loss of potential can be written in terms of the nodal degrees of freedom $\{q_d\}$ as

$$V_c^e=\frac{\lambda P_1}{2}\langle q_d\rangle\left(\int_0^{\bar{a}_c}\left[\frac{\partial\langle N_w\rangle^T_{z=0}}{\partial y}\right]\left[\frac{\partial\langle N_w\rangle_{z=0}}{\partial y}\right]dy\right)\{q_d\} \tag{9}$$

or

$$V_c^e=\frac{1}{2}\lambda\langle q_d\rangle\ [g_c]\ \{q_d\} \tag{10}$$

In a similar fashion, if a distributed load λw is applied $\bar{a}_d$ above the shear centre, then the loss of potential of the element V_d^e can be expressed as

$$V_d^e=\frac{\lambda}{2}\langle q_d\rangle\left(\int_0^L w\int_0^{\bar{a}_d}\left[\frac{\partial\langle N_w\rangle^T}{\partial y}\right]\left[\frac{\partial\langle N_w\rangle}{\partial y}\right]dy\ dz\right)\{q_d\} \tag{11}$$

where w may be a function of z. Eq.(11) may thus be written as

$$V_d^e=\frac{1}{2}\lambda\ \langle q_d\rangle\ [g_d]\ \{q_d\} \tag{12}$$

In formulating the element stability matrix, the geometric matrices $[g_c]$ and $[g_d]$ are merely added to the matrix $[g]$ in Eq. (4).

2.3. Modification for lateral-torsional buckling

The Bradford-Trahair element may be modified for lateral-torsional buckling, in order to achieve a comparison between the latter buckling mode and lateral-disortional buckling. For lateral-torsional buckling, the cross-section does not distort, and the buckling displacements may be expressed in terms of the lateral deflection u_L of the shear centre and the twist ϕ_L of the rigid cross-section. Provided that these are expressed as cubic polynomials in z, there are eight element degrees of freedom given by (Hancock and Trahair 1978).

$$\{q\}=\langle u_{L1},\ u_{L2},\ u'_{L1},\ u'_{L2},\ \phi_{L1},\ \phi_{L2},\ \phi'_{L1},\ \phi'_{L2}\rangle \tag{13}$$

Clearly for lateral-torsional buckling

$$u_L = \frac{u_T + u_B}{2} \tag{14}$$

and

$$\phi_L = \frac{u_T - u_B}{d_W} \tag{15}$$

where d_W is the depth of the web, taken here assuming thin-walled theory as the distance between the flange centroids. Hence from Eqs. (1), (13), (14) and (15)

$$\{q_d\} = [L]\{q_L\} \tag{16}$$

where $[L]$ is the 12×8 transformaion matrix given by

$$[L] = \begin{bmatrix} [I] & (d_w/2)[I] \\ [I] & (d_w/2)[I] \\ [O] & [J] \end{bmatrix} \tag{17}$$

in which $[I]$ is the 4×4 identity matrix, $[O]$ is the 4×4 null matrix, and where

$$[J] = \begin{bmatrix} 1 & 0 & 0 & 0 \\ 0 & 1 & 0 & 0 \\ 1 & 0 & 0 & 0 \\ 0 & 1 & 0 & 0 \end{bmatrix} \tag{18}$$

Hence the strain energy U^e and work done V^e for the element are, from Eqs. (3) and (4)

$$U^e = \frac{1}{2}\langle q_L \rangle \; [k_L] \; \{q_L\} \tag{19}$$

and

$$V^e = \frac{1}{2}\lambda \langle q_L \rangle \; [g_L] \; \{q_L\} \tag{20}$$

where the 8×8 stiffness and stabilty matrices for lateral-torsional buckling are respectively

$$[k_L] = [L]^T [k] [L] \tag{21}$$

$$[g_L] = [L]^T [g] [L] \tag{22}$$

The matrices $[k_L]$ and $[g_L]$ are obtained by pre- and post-multiplication of $[k]$ and $[g]$ respectively by computer. The assembly routine then follows that for lateral-distortional buckling, except of course that the global stiffness and stability matrices are of lower order than the corresponding global matrices for lateral-distortional buckling.

3. Buckling of overahanging beams

3.1. General

The finite element model described in the previous section was used to study the elastic lateral-

distortional and lateral-torsional buckling of the overhanging I-beam shown in Fig. 2. The span ratio L_b/L_c was kept constant at 2, while L_b/d_w was taken as 10. The entire beam *ABC* was discretised into fifteen equal length line elements, and the solutions for the buckling load were rapid on a personal computer using this meshing. The adopted Young's modulus was $E=200\times10^3$ MPa, and the Poisson's ratio ν was 0.3.

In calculating the buckling loads, the load P was placed at the tip of the cantilever segment on the top flange, at the shear centre or at the bottom flange. Lateral-distortional buckling loads are indicated by the subscript "*od*" and lateral-torsional bucking loads by the subscript "*ob*". Top flange loading is denoted by the superscript "*tf*", shear centre loading by the superscript "*sc*", while bottom flange loading is denoted by the superscript "*bf*", Hence, for example, P^{tf}_{od} would be the distortional buckling load for loading at the top flange.

The beam was simply supported with respect to out-of-plane buckling at *A*, and completely unrestrained at *C*. Two distortional buckling restraint cases were considered at the internal support *B*, *viz*. simply supported and partial, as shown in Fig. 1.

3.2. Buckling loads

Figs. 4 and 5 show the buckling loads for partial restraint at *B* for flange width to web depth ratios b_f/d_w of 0.1 and 0.2 respectively. The loads are normalised with respect to the lateral-torsional buckling load when the tip load is applied at the shear centre. Of course, for lateral-torsional buckling the web cannot distort, so that the partial support becomes a simple support.

It can be seen that for small values of the web to flange thickness ratios t_w/t_f, placing the load on the top flange decreases the buckling load well below that assuming shear centre lateral-torsional buckling, and even the reduction in bottom flange loading due to distortion is significant.

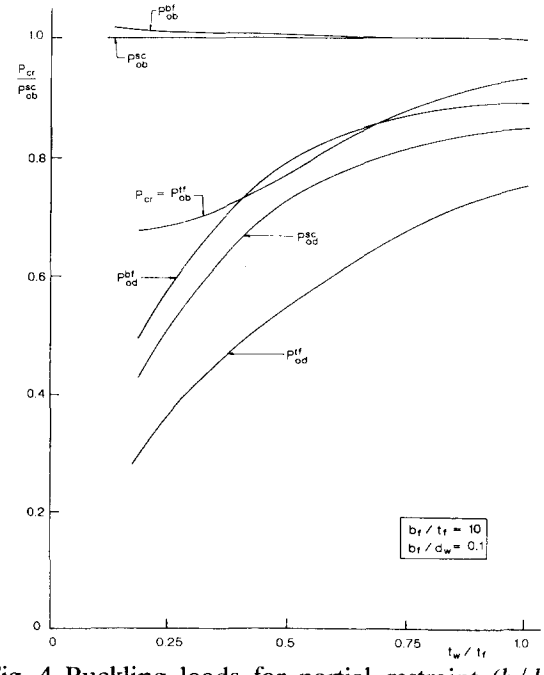

Fig. 4. Buckling loads for partial restraint ($b_f/d_w=0.1$)

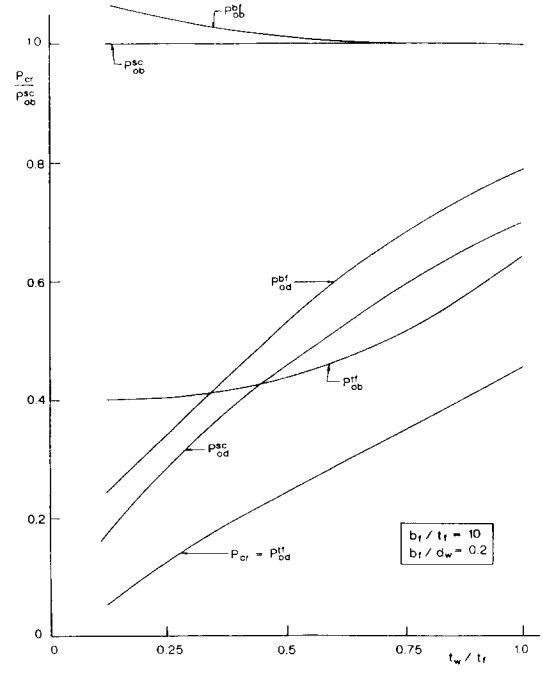

Fig. 5. Buckling loads for partial restraint ($b_f/d_w=0.2$)

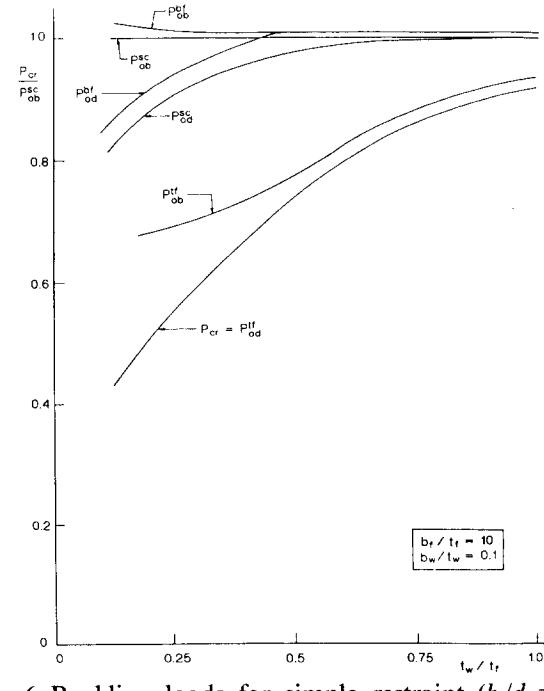

Fig. 6. Buckling loads for simple restraint ($b_f/d_w=0.1$)

The lateral-torsional buckling loads P_{ob} are also plotted, where it can be observed as expected that $P^{bf}_{ob}>P^{sc}_{ob}>P^{tf}_{ob}$

The effects of distortion are reduced as the web becomes less slender, i.e. when t_w/t_f is increased.

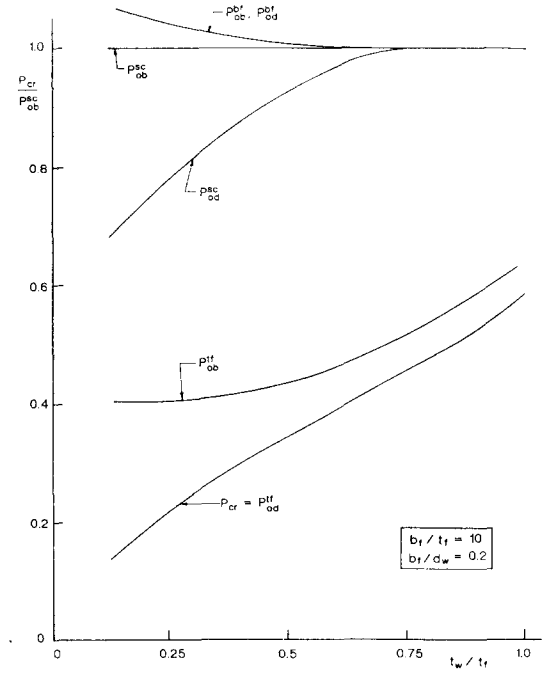

Fig. 7. Buckling loads for simple restraint ($b_f/d_w=0.2$)

This is also the case for the narrower flange ($b_f/d_w=0.1$ in Fig. 4), as against the wider flange with $b_f/d_w=0.2$ in Fig. 5. Moreover, the lateral-torsional buckling load P_{ob}^{tf} for top flange loading tends to approach its shear centre value for thicker webs.

The case of a simple support at B is illustrated in Figs. 6 and 7, which are the respective counterparts of Figs. 4 and 5. The effects of distortion during buckling are greatly reduced by fixing the top flange against lateral displacement and twist at the internal support. However, it can be seen that lateral-distortional buckling is still of consequence when the load is applied at the level of the top flange.

3.3. Buckling modes

The effect of partial restraint at B is illustrated by the buckled shapes in Fig. 8, which were obtained from the buckling eigenvector. Plot (a) in Fig. 8 is for lateral-torsional buckling with the load at the shear centre, while plot (c) is for lateral-torsional buckling with the load on the top flange. With shear centre loading, the bottom compressive flange in the internal span tends to displace significantly under lateral-torsional buckling, while for top flange loading it does not. Although subjected to tension, the top flange at the tip of the cantilever segment displaces more than the bottom flange under lateral-torsional buckling.

Fig. 8(b) shows the lateral-distortional buckling mode for shear centre loading, while the corresponding mode for top flange loading is given in Fig. 8(d). Also shown under these plots are the cross-sectional deformation at B and C. When the load is placed at the shear centre, the cross-section distorts at the internal partial restraint, but very little distortion takes place at the cantilever segment tip. On the other hand, placing the load on the top flange (Fig. 8(d)) accentuates distortion at the internal support, and substantial distortion occurs at the tip during buckling.

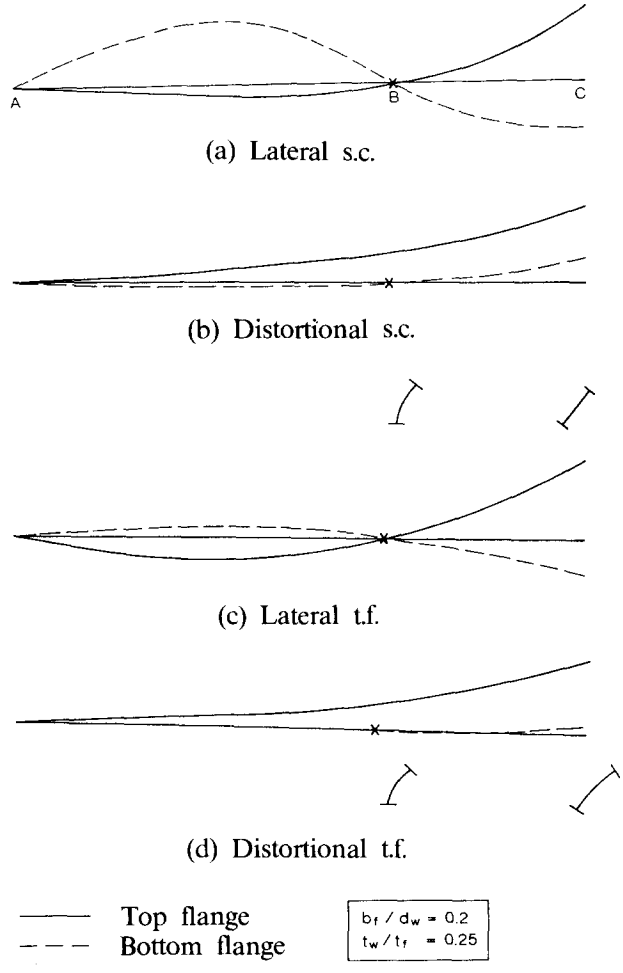

Fig. 8. Buckling modes

As with the lateral-torsional buckling case, there is much less bottom flange deflection during lateral-distortional buckling when the load is applied at the top flange compared with the deflections when the load is at the shear centre.

4. Concluding remarks

The Bradford-Trahair line element deployed for elastic lateral-distortional buckling of I-beams has been augmented to include loading within the cross-section but remote from the shear centre, and to model lateral-torsional buckling without distortion. The line element is very efficient, and is tractable on personal computers as the banded nature of the stiffness and stability matrices is utilised.

The finite element method was used to study the elastic overall buckling of overhanging beams in order to demonstrate the effects of load height and restraint at the internal support. When

the beam is only partially restrained at the internal support, distortion during buckling is very significant, especially when the load is applied at top flange level. This is evident from the buckling loads and mode shapes.

The study herein is only intended to shed lighton one situation wher distortion during buckling was tound to be significant. The augmented element may be deployed to investigate laterval-distortional buckling under a number of conditions of loading and restraint.

Acknowledgements

The author is grateful to Professor S. Kitipornchai of the University of Queensland for reading the manuscript.

References

Bradford, M.A. (1989), "Buckling of beams supported on seats", *The Structural Engineer,* **67**(23), 411-414.

Bradford, M.A. (1992a), "Lateral-distortional buckling of steel I-section members", *Journal of Constructional Steel Research,* **23**, 97-116.

Bradford, M.A. (1992b), "Bucking of doubly-symmetric cantilevers with thin webs", *Engineering Structures,* **14**, 327-334.

Bradford, M.A. and Trahair, N.S. (1981), "Distortional buckling of I-beams" *Journal of the Structural Division, ASCE* **107**(ST2), 355-370.

Hancock, G.J. and Trahair, N.S. (1978), "Finitie element analysis of the lateral buckling of continuously restrained beam-columns", *Civil Engineering Transactions, I.E.* Aust, **CE20**(2), 120-127.

Hancock, G.J., Bradford, M.A. and Trahair, N.S. (1980), "Web distortion and flexural-torsional buckling", *Journal of the Structural Division, ASCE*, **106**(ST7), 1557-1571.

Ronagh, H.R. and Bradford, M.A. (1996), "A rational model for the distortional buckling of tapered members", to appear in *Computer Methods in Applied Mechanics and Engineering.*

Trahair, N.S. (1983), "Lateral buckling of overhanging beams", *Proceedings of International Conference on Instability and Plastic Collapse of Steel Structures* (L.J. Morris ed.), Granada, London, 503-518.

Trahair, N.S. (1993), *Flexural-torsional buckling of structures,* Chapman and Hall, London.

Trahair, N.S. and Bradford, M.A. (1991), *The behaviour and design of steel structures, Revised 2nd edn.* Chapman and Hall, London.